ADVANCED ENERGY MATERIALS
www.advenergymat.de

Integratable Paper-Based Iontronic Power Source for All-In-One Disposable Electronics

Puguang Peng, Feiyao Yang, Zhonglin Wang, and Di Wei**

With the emergence of disposable electronics, compatible safe, flexible, and recyclable power sources have become a critical challenge. Here, an ultra-thin paper-based iontronic power source is enabled by highly efficient translational Li^+ transport within 2D nanofluidic channels of graphene oxide under a salinity gradient and the fine-tuned interfacial redox reactions. The paper-based source can generate volumetric power and energy densities of 438.02 mW cm^{-3} and 30.02 mWh cm^{-3}, respectively. Its areal power density is 1095.05 mW cm^{-2}, surpassing most flexible batteries. It maintains a working state when bent or even cut and can be simply recycled by incineration. By filling 2D nanofluidic inks in different pens, the power source can be drawn on paper when needed, which not only overcomes the inherent defect of self-discharge for most batteries but also enables writing directly on any insulating substrates. Furthermore, all-in-one disposable electronics comprised of an energy management system (paper-based triboelectric nanogenerator and iontronic power source) and wireless sensing system (temperature sensor with NFC circuits) are integrated onto one piece of paper by duplex printing, demonstrating the huge potential of such integratable iontronic power sources for soft, wireless, and conformable disposable electronics.

1. Introduction

Disposable electronics, such as e-skin,[1,2] e-tattoos,[3] e-textile,[4] and bioresorbable electronics,[5] are critical to acquiring more accurate data for bio-health monitoring[6] and enriching the Big Data for the ubiquitous Internet of Things (IoT). It is also especially important for the human-machine interface and in situ electrical stimulation in neuroengineering thanks to the flexible and degradable sensing platform.[7] Paper electronics as an essential type of disposable electronics have the unique advantages of biocompatibility, low cost, and recyclability.[8–11] Paper-based printed circuit boards (PCB),[12] field effect transistors,[13] antennas,[14] light emitting devices,[15] biosensors,[16] etc., have been reported recently. Additionally printing functional electronics on paper can also be converted to a variety of customizable shapes or Origami art forms to integrate devices in a compact space.[17–19] However, the Achilles heel for all disposable electronics lies in its compatible power supply. Although flexible energy storage devices, such as flexible lithium-ion batteries,[20,21] zinc-ion film batteries,[22,23] and high-power soft supercapacitors[24,25] were developed, they cannot be disposable due to safety and environmental reasons such as containing heavy metal hazards or toxic electrolytes. In addition, their fabrication process is also not coped with the disposable electronics. On the other hand, energy harvesting systems, such as acoustic energy harvesting,[26] sweat harvesting biosupercapacitor,[27] electromagnetic induction energy harvesting,[28,29] flexible photovoltaics,[30] evaporation-driven electrical generators,[31] piezoelectric and triboelectric nanogenerators (TENG),[32] are limited either by their low conversion efficiency, or discontinuous energy supply that is hardly used in practical applications. Thus, integrated energy management systems (i.e., integrated energy harvesting with energy storage units) for sustainable supply of direct current power are desperately needed, especially in driving the disposable multifunction integrated circuits (IC). Recently the key component of ICs, the microelectromechanical systems (MEMS) system, has been developed and used in ecoresorbable and bioresorbable medical devices, which is important to improve the human-machine interactive experience.[33] However, making a safe, ultra-thin, breathable, and recyclable energy management system on the disposable substrate could be hardly realized.

Energy from salinity gradient is a safe and biocompatible power existing in nature and living organisms but to put the osmotic power into pocket is a challenge due to the liquid reservoirs commonly used. In the last few years, portable osmotic power sources were reported to generate power through the

P. Peng, F. Yang, Z. Wang, D. Wei
Beijing Institute of Nanoenergy and Nanosystems
Chinese Academy of Sciences
Beijing 101400, China
E-mail: zhong.wang@mse.gatech.edu; weidi@binn.cas.cn
P. Peng
School of Nanoscience and Technology
University of Chinese Academy of Sciences
Beijing 100049, China
Z. Wang
School of Materials Science and Engineering
Georgia Institute of Technology
Atlanta, GA 30332, USA

The ORCID identification number(s) for the author(s) of this article can be found under https://doi.org/10.1002/aenm.202302360

DOI: 10.1002/aenm.202302360

rapid transport of ions in nanoconfined channels under salinity gradients that could be fabricated in small sizes and driven by humidity.[34–37] The nanoconfinement effect of the 2D nanofluidic channels enables highly efficient unipolar ion transport. When the size of the nanofluidic channel matches or is smaller than the Debye screening length (λ) of the ion, the ion selectivity and the kinetic path of ion diffusion tend to be significantly improved.[38,39] The surface charges on the inner walls of the nanofluidic channels can attract counter ions, and the strong ion-ion interactions lead to enhanced unidirectional diffusion, resulting in an increase in their ion transport conductivity by several orders of magnitude.[40] 2D nanofluidic materials such as graphene oxide (GO),[41,42] Mxene,[14] MoS_2,[13,43] etc., could be made in ink formula, easily processed, and demonstrated excellent mechanical flexibility.[44,45] Iontronics used ions as charge carriers and could avoid electrostatic and magnetic interferences. Till now, there are few reports on iontronics based on paper, which may be due to that the nature of paper would affect the ion transport channels to impair the function of iontronics for its uneven surface, easily deforming, and the functional groups in the cellulose chain, such as hydroxyl, carboxyl, and aldehyde groups.[46] The challenge is to construct stable nanoconfined channels on paper, and it may be addressed by choosing the most suitable paper through various characterizations to build stable ion transport channels. On the other hand, the unique advantages of paper such as printability, shearability, folding, and bending have not yet been fully exploited in iontronics.

In this paper, we present a printable, integratable paper-based iontronic energy management system for disposable applications. The carbon-based GO was chosen to provide 2D nanofluidic channels for disposable purposes. The compatibility (surface tension, wettability, etc.) of the GO inks with the selected tracing paper was fine-tuned and no negative effects were observed between the GO channels and the tracing paper interface. Therefore, the iontronic power source could be printed or sketched by three types of GO-based inks. In conventional osmotic power sources based on 2D nanofluidic materials, the energy is mainly determined by the asymmetric ion gradients, which face an unstable voltage output and low power density. Unlike conventional osmotic power sources, interfacial redox reactions were designed between the Ag electrode and the GO-based coating. In our iontronic energy storage unit, the Li^+ transport within 2D nanofluidic channels of GO under salinity gradient together with the tailored interfacial redox reactions achieved a high volumetric energy density of 30.02 mWh cm^{-3} and power density of 438.02 mW cm^{-3}, which are capable to power most electronics. It provides a versatile way to print/write energy sources on PCBs directly, for example, such a unit could be sketched on paper powering LED and other circuits connected simply by pencil drawing. The ultrathin paper-based iontronic energy storage unit maintains functioning when being bent or even cut, and could be recycled by incineration. Its nontoxicity can further broaden the disposable applications in health monitoring via direct skin contact to improve the human-machine interface experience. Combining with the TENG energy harvester, the self-driven integrated energy management system in a piece of paper could be realized to suppress the self-discharge of the iontronic energy storage unit to a certain extent, greatly extending the energy supply lifetime. Furthermore, all-in-one disposable electronics on one piece of paper was demonstrated, consisting of a printable iontronic power source, paper-based TENG energy harvesting unit, and printed circuits of a temperature sensor with NFC antenna, which shows great potential in a wider range of applications in disposable electronics.

2. Results and Discussion

2.1. The Planar Paper-Based Iontronic Power Source

Paper as a carrier of civilization records and enables a prominent spread of technology and ideas for humans. In the electronic age, paper is one of the most cost-effective materials (0.1 cent dm^{-2}) as compared to polymer substrates such as polyethylene terephthalate (≈2 cent dm^{-2}) and polyimide (≈30 cent dm^{-2})[8] for printable electronics. It was an ideal substrate candidate for a disposable power source, but the compatibility between ink and paper always needs to be fine-tuned.[14,47] Herein, the carbon-based GO ink was chosen due to the convenience of tailoring its physiochemical properties for printing. **Figure 1**a and Figure S1 (Supporting Information) showed the working principle of the iontronic power source and the all-in-one disposable electronics on paper with its integratable energy management system that could be prepared by printing or writing and its wireless sensing system, both on paper. To realize the paper-based iontronic power source, three inks were used in the printing process, noted as GO ink, $AgNO_3$ ink, and LiI-rGO ink, respectively. The 2D nanofluidic material of GO was prepared from the modified Hummer's method and obtained after subsequent freeze-drying (Figure S2a–f, Supporting Information). After that, it was dispersed in a solution of deionized water and ethanol (V_{water}:$V_{ethanol}$ = 4:1) to form a GO dispersion of 10 mg mL^{-1}. The purpose of using ethanol is to dry the ink quickly when printing, which could also prevent the penetration and diffusion of the GO ink on paper and improve printing resolution. In parallel, GO ink was dispersed by intermittently ultrasound sonication for 5 min to optimize the rheological properties to fit the extrusion printer. After ultrasound sonication, the flake size of GO was dramatically reduced but more monolayer structures were present (Figure S3a,b, Supporting Information). The average flake size of these GO nanosheets is ≈0.5–1 µm in diameter and 1 nm in thickness (Figure 1b,c). Because of the abundance of hydrophilic functional groups on the GO surface, the GO ink had an ideal shear-thinning viscosity/elasticity profile (with a viscosity of 90 Pa s), allowing continuous printing and fast curing (Figure 1d,e). Figure S4 (Supporting Information) further demonstrates the rheological properties of GO ink. In addition, the prepared GO ink can be stored for a long time at low temperatures (<4 °C) without agglomeration or chemical changes after at least a year (Figure S5, Supporting Information), which may be due to the small, uniform particle size and large monolayer ratio (>70%) of GO. Such GO ink had excellent adhesion and could be directly printed on different papers by a three-axis mechanical pneumatic liquid extrusion printing system and built large area of lateral 2D nanofluidic channels (Figure 1f,g; Figure S6, Supporting Information), which facilitated the fast translational transport of cations. Such a printing system is equipped with a suction module to enhance the printing resolution by balancing the gravity of inks during printing. Different paper substrates, such as photo paper,

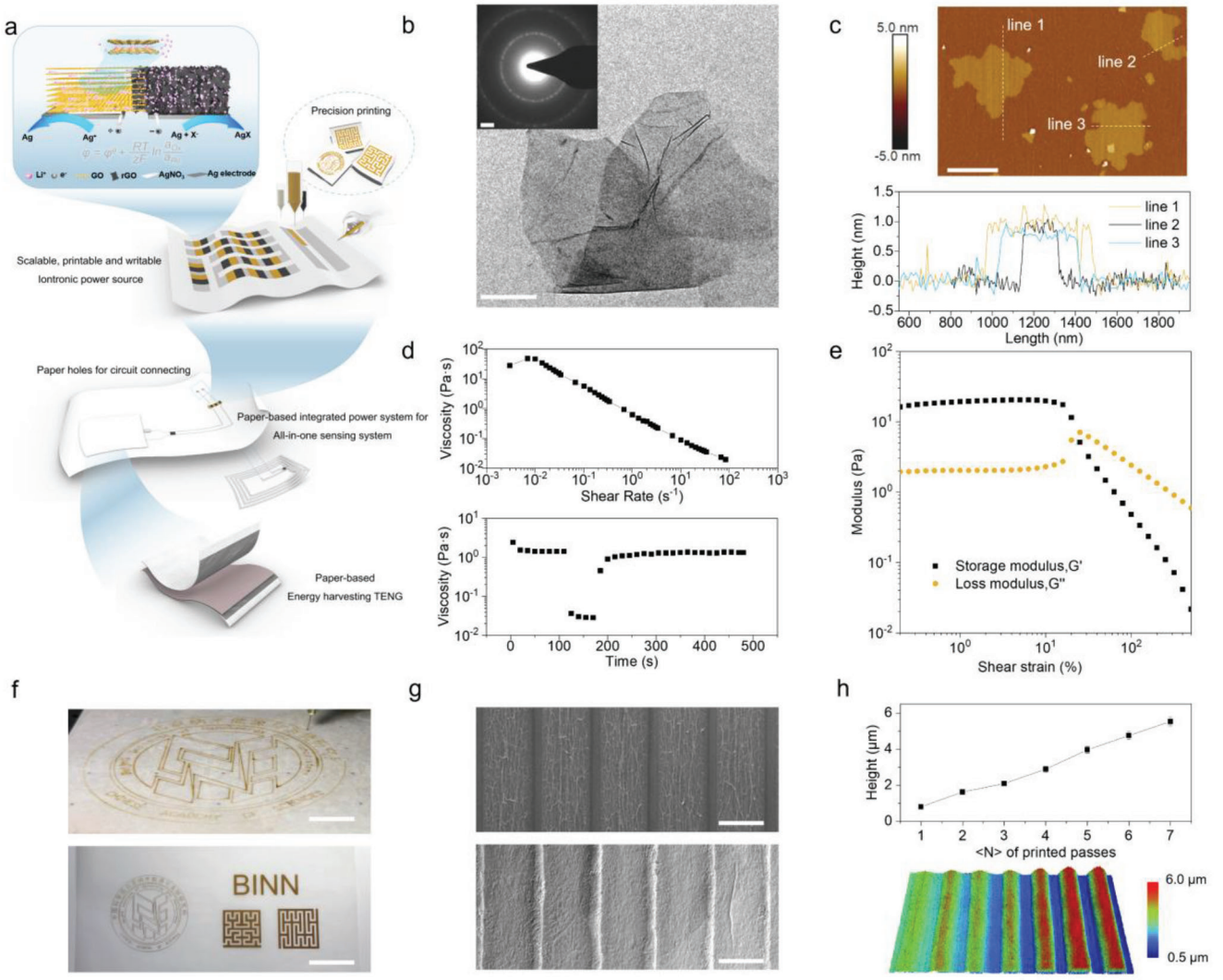

Figure 1. Characterizations and the direct printing of the fine-tuned GO ink. a) Schematic illustration of direct printing of GO-based inks supported for iontronic power source and its mechanism, and the integratable energy management system for all-in-one disposable applications. b) Transmission electron microscopy (TEM) image of a piece of GO layer. Scale bar: 500 nm. Inset: the selected area electron diffraction (SAED) pattern. Scale bar, 2 1/nm. c) Atomic force microscopy (AFM) image of GO layers and corresponding height profiles. d) Rheological properties of GO ink with viscosity plotted as a function of shear rate (top) and interval shearing time (bottom, alternating the shear rate between 0.1 and 100 s^{-1} to simulate the extrusion process). e) Storage modulus (G') and loss modulus (G'') of the GO ink versus shear stress. f) Top: optical image of high-resolution direct extrusion printing for GO. Scale bar, 2 cm. Bottom: optical image of GO circuits fabricated by extrusion printing. Scale bar, 5 cm. g) SEM image of the printed GO lines in PET (top) and tracing paper (bottom) with a gap of 100 μm. Scale bar, both 1 mm. h) Thickness (top) and surface profiles (bottom) of the printed GO lines as a function number of printing times, <N>.

tracing paper, filter paper, copy paper, polypropylene paper, and kraft paper were characterized (Figure S7, Supporting Information), showing continuous and stable print paths. However, the initial droplet aggregations may stem from the lack of coordination between air pressure and machine movement at the start-up. Almost all commercial papers have good wetting properties for GO inks with contact angles of less than 90°, probably due to the porous and rough morphology of the paper surface (Figures S8 and S9, Supporting Information). It is worth noting that although Raman and IR spectroscopy tests showed essentially the same spectral image on the printed GO on different paper substrates (Figures S10 and S11, Supporting Information), most paper substrates such as photo paper and copy paper are coated with calcium carbonate (Figure S12, Supporting Information) that is detrimental to the electrochemical performance of the iontronic power source. Therefore, tracing paper without any calcium carbonate coating was chosen as the substrate and it has been verified to be breathable as shown in Figure S13 (Supporting Information). In addition, GO was first printed on the Polyethylene terephthalate (PET) substrate as a benchmark to illustrate the printing resolution, and good resolution was also obtained when it was printed on tracing paper (Figure 1g). Further horizontal SEM images also showed the 2D nanofluidic channels of GO printed on tracing paper could also be constructed

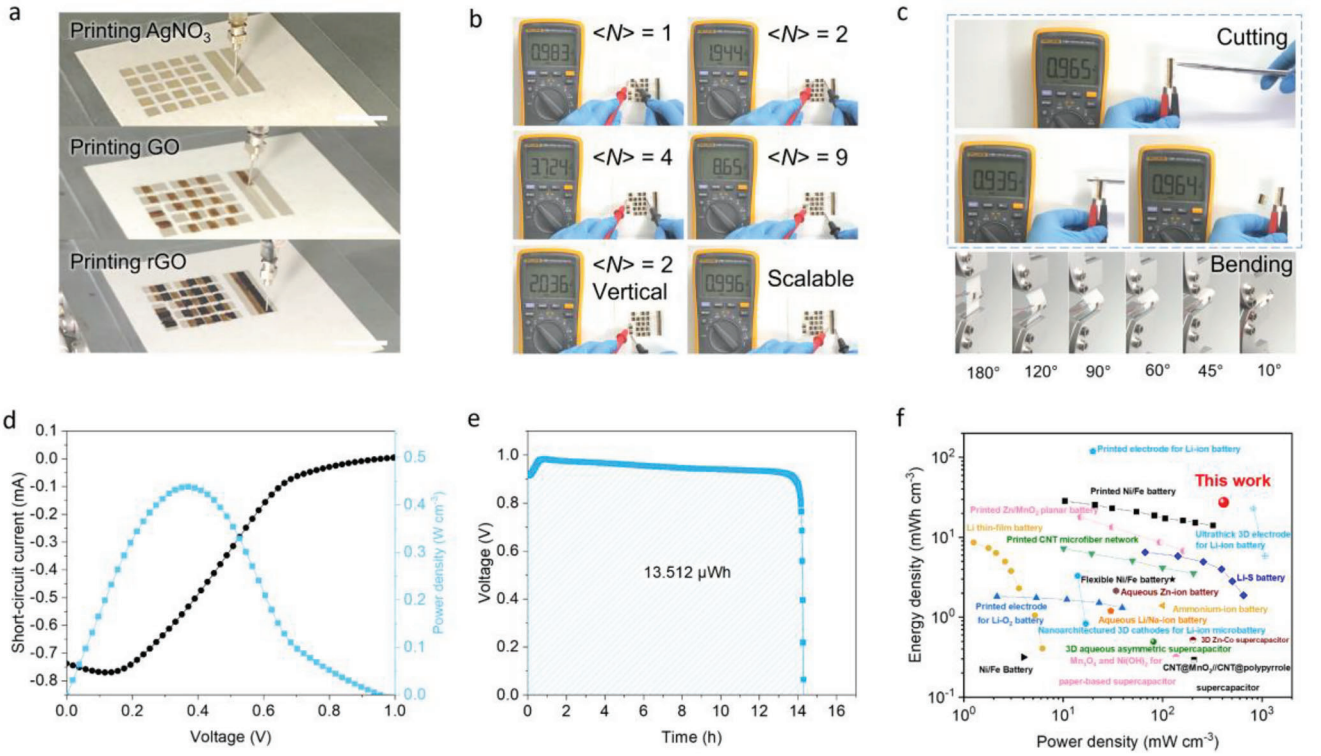

Figure 2. The direct printing of the iontronic power source and its characterizations. a) Optical image of high-resolution extrusion printing to fabricate customized iontronic power source with different <N> of units or lengths. Scale bar, 1 cm. b) Optical image shows the V_{oc} of customized iontronic power source with different <N> of units or lengths. c) Cutting (top) and bending (bottom) test of the iontronic power source. d) *I–V* characteristic and the corresponding power density of the smallest iontronic power source at 25 °C, RH 80%. e) The discharge curve of the iontronic power sources at 1 μA, 25 °C, RH 80%. f) Comparison of energy and power density of the iontronic power source in the Ragone plot (Data from Table S2, Supporting Information).

successfully (Figure S14, Supporting Information). GO lines with precise patterns of 50–150 μm can be printed directly (Figure S15a,b, Supporting Information), and excellent precision is important for preventing internal short circuits in planar iontronic power sources. The high printing resolution could be attributed to the effective strength modulus of the hydrophilic GO ink, allowing the ink to retain its shape and not spread after printing. Measured by an optical 3D profilometer (Figure 1h; Figure S16a,b, Supporting Information), the printed lines of the GO ink showed a sharp profile with an elliptical cross-section. In addition, the effective length of the printed circuit can be extended by space-filling curves (Figure S17, Supporting Information) or by using the art of origami to extend the application into three dimensions. The superior rheological and mechanical properties of GO ink allow it to be used in fully printed iontronic power sources. Therefore, we modulated $AgNO_3$ ink and LiI-rGO ink on this basis, and the corresponding rheological performance tests and physical characterization showed similar printing performance to that of the GO ink (Figure S18a–f, Supporting Information).

The paper-based planar iontronic power source could then be printed in high resolution with miniature cells in series or parallel, as shown in Video S1 (Supporting Information) and schematic photos in **Figure 2**a. The cells can be arranged arbitrarily, horizontally or vertically, in the front or back of the paper, to meet customized energy needs. The unit cell 10 mm in length and 5 mm in width has two Ag electrodes (4 mm × 5 mm for each part), which were first screen-printed side by side on a paper plane. Then $AgNO_3$ ink, GO ink, and LiI-rGO ink were printed by the extrusion printer from left to right in that order. Each ink was printed twice, and the thickness of the device obtained by surface profiler testing was ≈17.5 μm (Figure S19a–d, Supporting Information), which is consistent with previous pure ink printing results as shown in Figure S16 (Supporting Information).

The open-circuit voltage (V_{OC}) generated by a unit of the iontronic power source printed on paper can reach 0.963 V (25 °C 60% RH), and higher voltages can be obtained for the units connected in series as shown in Figure 2b. The voltage was increasing sequentially depending on the number of printed units, where 2 units connected in series could generate ≈2 V (up to 1.944 V in horizontal or 2.036 V in vertical directions), 4 or 9 units connected in series could approach 3.724 or 8.65 V, respectively, and higher voltage of 20 V could be obtained when 20 units were connected in series, which can satisfy most portable electronics (Figure S20a, Supporting Information). Meanwhile, with the increasing printed length of the device (equivalent to cells connected in parallel) from 1 to 29 cm (length of a copy paper), they exhibited an almost linear trend of growing I_{SC} up to 40 mA as shown in Figure S20b (Supporting Information). This shows the low internal resistance of ionic power source due to the efficient

Li^+ transport inside 2D nanofluidic channels of GO and offers a versatile and convenient design of battery pack by printing them in various designs. In addition, the unique advantage of a paper-based power source is that it can be printed on large flat surfaces or integrated and applied in 3D space through Origami/Kirigami, which can satisfy the energy needs of various electronic devices. As shown in Figure 2c, the voltage of the cell remains almost the same after cutting without the risk of short circuit or burning, demonstrating great safety and environmental significance. Paper-based iontronic power sources can also accommodate arbitrary bending with little effect on their current output, with only ≈12% attenuation in I_{sc} even nearly fully bent (10°, as shown in Figure 2c bottom; Figure S21, Supporting Information) which is important for the integration of flexible electronic devices.

According to the Nernst equation, the V_{oc} of the redox couple between Ag/Ag^+ and Ag/AgI can be calculated as 0.95 V, while the value of a unit cell is slightly higher than the calculated one because it also included the voltage from salinity gradient (Figure S22, Supporting Information). Further linear sweep voltammetry test (LSV) also obtained the V_{oc} value of 0.996 V at a sweep rate of 0.01 V s^{-1} and the iontronic power source could reach a short-circuit current (I_{sc}) of 700 µA, with a calculated power density of 438.02 mW cm^{-3} in volumetric and 1095.05 mW cm^{-2} in areal (Figure 2D; Note S1, Supporting Information). It can also be discharged at a current of 1 µA with an energy density of up to 30.02 mWh cm^{-3} (Figure 2e; Note S1, Supporting Information). The traditional osmotic power source was based on the salinity gradient from reservoirs on both sides of the membrane and is essentially an energy harvesting method, impractical to be used in portable electronics (Table S1, Supporting Information). By coupling the chemical redox reactions at the electrode interface and transporting the Li^+ through the 2D nanofluidic channels, high ionic power could be stored on a piece of paper. It also showed a perfect reversible redox peak in cyclic voltammogram, and the galvanostatic charge-discharge test proved it can be recharged up to 30 cycles before over-discharging (Figure S23, Supporting Information). Such paper-based ionic power source eliminates the risks of explosion or environmental contamination and its volumetric energy density is comparable to printed silver-zinc, thin-film lithium batteries, and other energy storage devices as shown in the Ragone plot (based on the total volume of the device, Figure 2f; Table S2, Supporting Information).

The working mechanism of the ionic power source is illustrated in Figure 1a. The 2D nanofluidic channels of GO would effectively transport Li^+ cations under humidity and the migration of Li^+ was evidenced by characterizations in Figure S24 (Supporting Information). The LiI-rGO containing a large amount of Li^+ functions as the anode in the iontronic power source and the electrode containing $AgNO_3$ was the cathode. In this case, the ionic current was generated inside the cell by capturing the moisture in the environment, and it could be expected to connect the electrochemical reaction on the electrode surface to realize the combined current of iontronics and electronics. The paper-based power source may undergo a reduction of $Ag^+ + e^- \rightarrow Ag$ at the cathode and an oxidation of $Ag + I^- \rightarrow AgI + e^-$ at the anode (with the surplus iodine ions involved in this process). An optical microscope recorded the occurrence of this process in situ and observed Ag metals at the cathode and some white crystals at the anode (Figure S25, Supporting Information), where the white crystal was verified as AgI by X-Ray Diffraction (XRD, Figure S26, Supporting Information) and Energy Dispersive X-Ray Spectroscopy (EDS, Figure S27, Supporting Information).

2.2. Paper-Based Integrated Energy Management System

A fully paper-based integrated energy management system including energy harvesting and storage units was built as illustrated in **Figure 3**a. It could be applied to meet the output requirements of wearable and disposable electronics to extend their operation time. The natural breathability of the paper allows the printable iontronic power source to contact the skin directly for a long time even under deformation (Inset photo in Figure 3a). In energy harvesting, the porous rough surface and the shape-adaptive design of paper make it well suited for triboelectric nanogenerators (TENG), which are able to harvest frictional energy from various types of human mechanical motions (such as stretching, squeezing, and twisting) to replenish the planar iontronic power source to extend its service time.

The paper-based TENG (P-TENG) consists of two layers, the charge-collecting electrode layer was made by drawing graphite on tracing paper using a soft charcoal pencil and the friction layer refers to the Poly Tetra Fluoro Ethylene (PTFE) film as shown in Figure 3a and Figure S28 (Supporting Information). Both layers with similar areas (10 cm × 10 cm) were used in the P-TENG and they can be placed in easy-to-friction locations in the body, such as the underarm to generate continuous alternative current (AC) electrical output. A rectifier bridge was used to convert AC to direct current (DC). To evaluate the electrical output performance of the P-TENG, a linear motor was used under a low-frequency motion to simulate the contact separation process like human motion. The transferred charge (Q_{sc}), open-circuit voltage (V_{oc}), and short-circuit current (I_{sc}) generated by the P-TENG were tested at five progressive frequencies from 1 to 5 Hz. The variation trends of V_{oc}, I_{sc}, and Q_{sc} can be explained by Maxwell's displacement current[32] (Note S2, Supporting Information). As shown in Figure S29 (Supporting Information) and Figure 3b, the Q_{sc} and V_{oc} of the P-TENG can be maintained at ≈85 nC and 70 V almost independently under variable frequency. In contrast, the maximum I_{sc} was obtained at 5 Hz of 30 µA (Figure 3c), and it could charge a 100 µF capacitor to 1.5 V within 100 s (Figure 3d) with a bridge rectifier. Furthermore, the output performances under different humidity conditions, RH of 20%, 40%, 60%, and 80% were tested for the P-TENG as shown in Figure S30 (Supporting Information). It was shown that the P-TENG can maintain its output until RH 60%, only under the very high humidity (RH 80%), the output of the P-TENG will be reduced. When the P-TENG was in operation, the voltage of the paper-based integrated energy management system (including P-TENG and iontronic power source with a V_{oc} of ≈0.98 V) would be kept above the V_{oc} (Figure 3e), which means the P-TENG can effectively charge the iontronic power source. This profile is consistent with the above results of its charging characteristics by the electrochemical workstation as shown in Figure S23 (Supporting Information). Such an integrated energy management system can discharge continuously for more than 25 h at a current of 1 µA, with

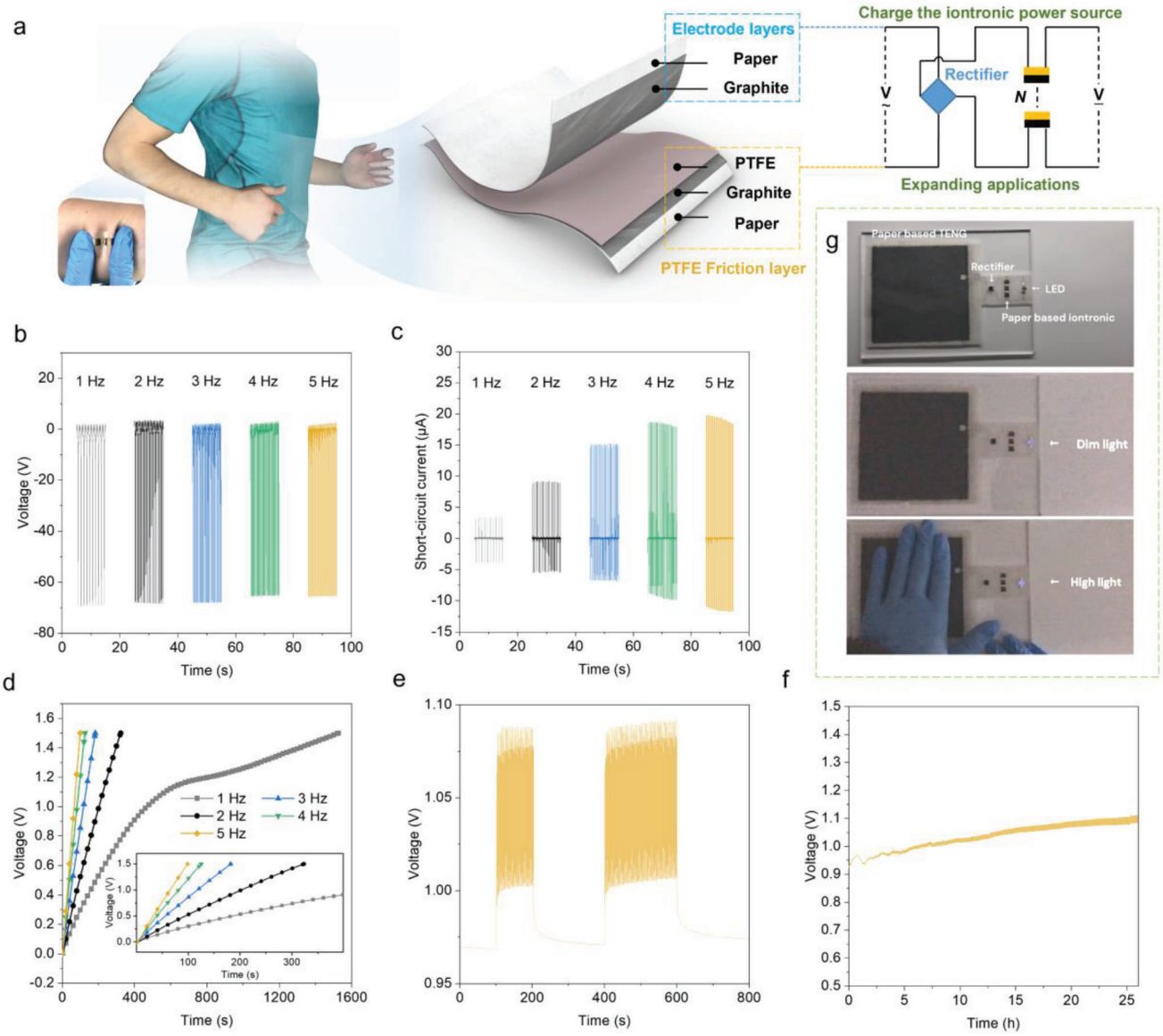

Figure 3. The energy harvesting TENG for the smart integratable energy management system. a) Schematic illustration of the application and structure of the TENG and the equivalent circuit for it to charge the iontronic power source, such iontronic power source can be safely attached to the surface of human skin (inset photo) and integrated with the TENG to build an integrated energy management system. b,c) The output of (b) V_{oc} and (c) I_{sc} at different frequencies. d) Charging a capacitor (100 μF) to 1.5 V by the paper-based TENG at different frequencies, inset: the enlarged pattern of the charging curves. e) The chronopotential test of the iontronic power source charged by the TENG at 5 Hz. f) The galvanostatic discharge performance of the iontronic power source integrated with TENG at 1 μA. g) Paper-based energy management system made of TENG and iontronic power source could light up LED.

60% higher energy than discharging the iontronic power source alone, as shown in Figure 3f. During human movement, the body frequency sometimes can even exceed 5 Hz, which is expected to generate more energy. Such a paper-based energy management system could boost up lightening of LED as demonstrated in Video S2 (Supporting Information) and Figure 3g, showing the capability of continuously charging the battery that can broaden the perspective applications in many electronics. It is particularly important to increase the service time of disposable electronics, especially vital for long-term and high-precision medical monitoring applications.

2.3. All-In-One Disposable Electronics on Paper

The ink form of 2D nanofluidic materials provides a platform for convenient modification of surface charge and rheology. Sketching power sources with such inks provides not only a versatile method to integrate energy units with the PCB board for various IoT applications (**Figure 4**a) but also a new way to store energy. When the power source was sketched, the battery was embedded in the same plane of PCB. As Figure 4b and Video S3 (Supporting Information) show, four paper-based iontronic power sources were first sketched on a piece of paper. If connected in series, it

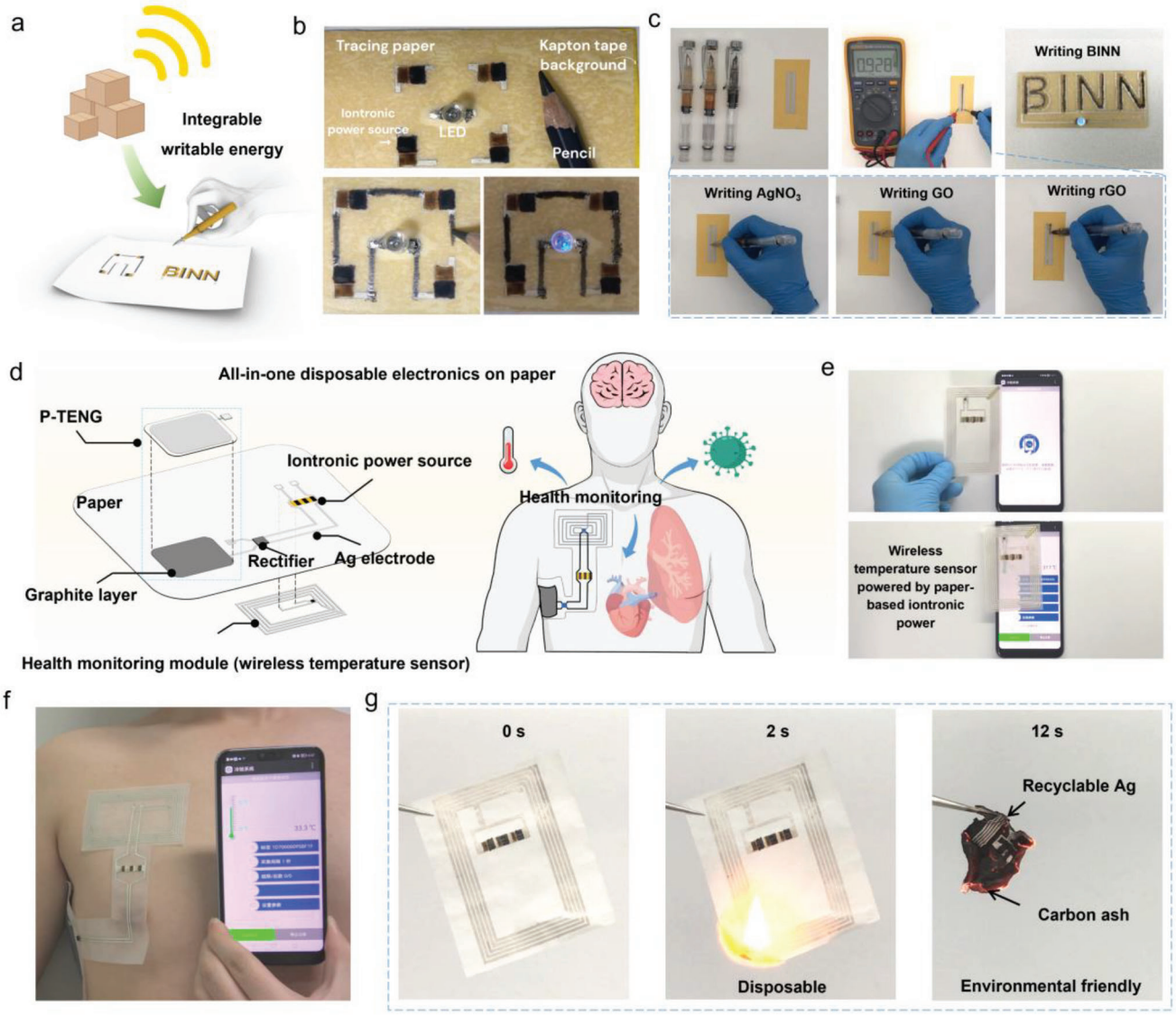

Figure 4. The integratable power for an all-in-one disposable self-driven sensing system. a) Schematic illustration of the integratable power realized by writing. b) The iontronic power circuit connected by pencil sketch c) the iontronic power unit sketched on paper that can provide a normal voltage and light up the LED. d) Schematic illustration of the all-in-one disposable electronics for wireless health monitoring. e) Driving the paper-based wireless temperature sensor by iontronic power source. f) Paper-based all-in-one disposable electronics directly attached to the human body. g) Recycle of the paper-based iontronic power source and printed electronics by incineration.

could generate a voltage over 3.5 V, which can meet the normal operating conditions of the commercial LED. It was shown that the easy interconnection of iontronic power sources by a pencil avoids the use of metal wires or other printed charge collectors to connect functional devices. Such writable/erasable connection optimizes the switching units in the circuit and has important applications for rapidly building larger and smarter ICs. Using the pens filled with different functional inks, an iontronic power source could be sketched directly on paper or any insulating substrates. A portable power source can be quickly sketched without influence on its voltage performance by pens filled with $AgNO_3$, GO, and LiI-rGO ink (Figure 4c; Video S4, Supporting Information). It showed the V_{oc} of ≈0.928 V which is consistent with the previous printed one. Such a new way to store energy in pens could overcome the inherent defect of self-discharge for most batteries, where discharge happens as soon as the battery is assembled. To demonstrate the practical application of the writable power source, the four letters "BINN" were sketched on a paper substrate to form a series of four units and then dried under ambient conditions. The sketched power source can light up the LED stably and provides a low-cost, portable manufacturing route for coupling energy units with printed electronics or disposable electronics on the same substrate.

Till today, there was no report on printing integrated energy management systems and ICs on the same piece of paper with a thickness of ≈10 µm. A wireless skin-interfaced disposable temperature sensor was demonstrated here. A duplex printing strategy was used and the energy management system on one side

is connected to the wireless sensing module by Ag ink through the plated-through-holes (PTH) technique as in the processing of PCBs (Figure 4d). Specifically speaking, the integrated energy management system was printed on one side of the paper, which consisted of P-TENG and an iontronic power source. A wireless temperature sensing module was printed on the other side of the paper and the electrodes were connected to the energy management system through the small holes in the paper. The wireless temperature sensing module was made up of a Microprogrammed Control Unit (MCU) and a standard five-antenna near-field communication (NFC). Its internal sensing chip circuit is shown in Figure S31 (Supporting Information), and the temperature data need to be refreshed and recorded by an external energy source. Although such a sensing unit is functional when only driven by an iontronic power source (Figure 4e; Video S5, Supporting Information), the integrated P-TENG extended its service life as demonstrated previously. Thanks to the extraordinary biosafety and ultra-thin properties of the iontronic power source and the breathability of the paper substrate, this all-in-one disposable wireless sensing system can be appended directly to the human skin (Figure 4f; Figure S32, Supporting Information). It can continuously monitor the body temperature, which is important to reduce the cost of identifying early inflammation during epidemics, such as COVID-19. In addition, the paper-based iontronic power source doesn't contain heavy metals or toxic electrolytes and could be recycled by incineration (Figure 4g), which is one of the most ideal and effective ways to recycle the electrochemical energy storage devices. Ag can be separated directly from the burned ash due to its non-burnable nature, while Li^+ is soluble and can be recycled from liquid waste.

3. Conclusion

Disposable electronics does not simply mean to be mechanically flexible just by virtue of thin geometry. All electronics need power and it offers more challenges on biocompatibility, breathability, and recyclability, on top of which, building a power source to meet all these requirements is a more challenging task. This paper is the first report to demonstrate integrated energy management systems and ICs by duplex printing on one piece of paper. 2D nanofluidic channels in the GO could enable highly efficient unipolar ion transport of Li^+. Coupling the salinity gradient-driven redox reactions on the Ag electrode, the paper-based iontronic power source generated volumetric power and energy densities of 438.02 mW cm^{-3} and 30.02 mWh cm^{-3}, respectively. Its areal power density is 1095.05 mW cm^{-2}, surpassing most flexible batteries as compared in the Ragone plot and Tables S1 and S2 (Supporting Information). It can be easily integrated with energy harvesting systems like P-TENG to form a fully paper-based energy management system to continuously power disposable electronics. The paper's natural breathability and biocompatibility allow direct skin contact. A skin-interfaced all-in-one disposable electronic on paper was demonstrated and attached to the human body to offer wireless temperature monitoring in situ. It offers a new paradigm to integrate printable iontronic power with functional ICs, which can be either printed on one side of the paper or on a double side of the paper connecting through the PTH technique. The all-in-one paper-based disposable electronics could be easily recycled simply by incineration. In addition, the three GO-based inks offer versatile ways to provide energy. The iontronic power source could be easily scaled on paper substrate by printing, and be printed/sketched directly on the PCBs or any insulating substrate. Filled with different types of inks in pens, the power unit could be sketched in circuits on paper. Such a new way to store inks in different pens could also overcome the inherent defect of self-discharge for most batteries, where discharge happens as soon as the battery is assembled. Storing iontronic power in one piece of paper could open a new scenario for paper-based diagnostic systems that are currently mainly engaged with passive detection without a power supply.[48,49] It will offer broader perspectives on the next generation of IoT, bio/health in situ monitoring/diagnostics, smart logistic systems, deploying in future human-machine interfaces, and neuromorphic computing.

4. Experimental Section

Material Preparation and Experimental Methods: This research complies with all relevant ethical regulations oversight by the Beijing Institute of Nanoenergy and Nanosystems, Chinese Academy of Sciences.

Preparation of GO Powder and the GO Ink: GO was prepared from graphite powders (XFNANO, INC) using a modified Hummers method. Graphite powders (1 g), H_3PO_4 (2 mL), and H_2SO_4 (21 mL) were premixed in an ice water bath, afterward the $KMnO_4$ (3 g) was slowly added to react for 2 h. Then the solution was transferred to a 35 °C thermostatic water bath and stirred for ≈0.5 h to form a thick paste. After that, 46 mL of deionized (DI) water was slowly added and transferred to a 95 °C thermostatic water bath for 15 min. Finally, 140 mL of water and 10 mL of H_2O_2 (30%) were added. After washing away soluble salts and incompletely reacted graphite by centrifuge, the GO powder could be finally obtained from the GO dispersion by freeze-drying.

The GO ink was prepared by dissolving different weights of GO powder in a 20 mL solution of DI water and ethanol (V water: V ethanol = 4:1) with ultrasonic operation to form GO inks with various concentrations.

All related chemicals of H_2SO_4, $KMnO_4$, H_2O_2, and H_3PO_4 were purchased from Sigma–Aldrich and were used as received. DI water with a resistivity of above 18 $M\omega$ cm^{-1} was collected from a Mili-Q Biocel system.

Preparation of $AgNO_3$ Ink and LiI-rGO Ink: The $AgNO_3$ ink was prepared by mixing 3.397 g of $AgNO_3$ and 20 mg GO powder in 20 mL DI water with ultrasonic operation, where the GO powder was used to regulate its rheological properties.

The LiI-rGO ink was prepared by adding 2.677 g of LiI and 10 mg GO powder in 20 mL DI water with ultrasonic operation before incubating it at 60 °C for 24 h.

Screen Printing of the Ag Electrode: Screen printable Ag ink, purchased from Changsung, was printed on commercial papers including copy paper, tracing paper, photo paper, filter paper, polypropylene paper, and kraft paper, by using the predesigned screen-printing patterns. The obtained substrates were dried in an oven at 130 °C for 30 min.

Precision Extrusion Printing of the Inks: The three-axis mechanical pneumatic liquid extrusion system from Fairchild Industrial Products Company, USA was used to extrusion print the GO, $AgNO_3$, and LiI-rGO inks. It is capable of carrying the pneumatic extrusion nozzle according to the preset program to create specific patterns on substrate surfaces accurately.

Fabrication of the Paper-Based TENG: The paper-based TENG was prepared by using a soft charcoal pencil to draw a 10 cm × 10 cm pattern on two pieces of paper, with the designed screen-printed Ag electrodes, and one of the drawn papers was coved with a PTEF layer to form the friction section and the other was the conductive section. After that, these two papers were laminated together and a rectifier bridge for AC to DC conversion to fabricate a paper-based TENG was combined.

Fabrication of the All-In-One Disposable Electronics on Paper: The paper-based all-in-one disposable electronics were fabricated on a piece of paper by screen printing the designed Ag electrodes first on the different sides of this paper. One side of the paper is a part of the paper-based TENG for energy harvesting and then extrusion printing the iontronic power source to store the electronic energy to form the energy management system. Meanwhile, the plated-through holes (PTH) technique was used to connect the wireless temperature sensing module on the other side of the paper. It is noticed that the wireless temperature sensing module was also made up of a printed standard five-antenna near-field communication (NFC) and a Microprogrammed Control Unit (MCU, AS39513, Advanced Monolithic Systems Inc., USA), therefore, the all-in-one disposable electronics could be fabricated by simply printing, drawing and assembling.

Characterization and Measurements: Morphologies of GO powder and paper-based iontronic power source are observed by the SEM (SU8020, Hitachi) with the 5.0 kV accelerating voltage, 10 μA emission current, and TEM (FEI Titan, USA) with the operating voltage of 300 Kv. Meanwhile, the Energy Dispersive X-ray (EDX) test from SU8020 was used for the element analysis. Atomic force microscopy (AFM) images were taken by a Dimension Icon AFM (Bruker AXS, Germany) in peak force tapping mode under ambient conditions. X-ray diffraction (XRD) patterns were acquired through a Bruker D8 Advance Diffractometer (Germany) with a working voltage of 40 kV. The Dektak XT stylus profiler (Brucker) was used to profile the morphology of the printing lines of GO ink, $AgNO_3$ ink, and LiI-rGO ink as well as the whole device, which provided information on volume values for the calculation of specific energy and power density. The infiltration ability of each ink was characterized by a surface tension meter (Dataphysics OCA20, Germany). Raman spectra were collected with the LabRAM HR Evolution (Horiba) with a 532 nm laser. FTIR was collected by Bruker VERTEX80v. Zeta potential was obtained by using a Beckman coulter instrument (Delsamax Pro). Particle-size analysis was measured with BLUEWAVE S3500 (Microtrac) with a 408 nm laser. The rheological property of the inks was measured with an Anton Paar MCR 301 rheometer under the parallel plate geometries with a diameter of 25 mm and a gap of 0.5 mm.

Electrochemical Measurements and Humidity Control: The electrochemical measurements, unless otherwise stated, were carried out with the electrochemical workstation (Multi Autolab M204) in the Voetsch 4018C environmental chamber to control temperature and relative humidity (RH). For the paper-based TENG characterization, a step motor (LinMot E1100) was used to provide the input of mechanical motions. The voltage and current output were recorded by a Keithley electrometer 6514. The LED was purchased from JENSHEN, China, to show the potential application of the iontronic power source and paper-based TENG.

Mechanical Flexibility Measurement of the Iontronic Power Source: A microcomputer-controlled electronic universal testing machine, MTS EXCEED Model E 43, USA, was used to test the mechanical flexibility of the paper-based iontronic power source, and two Ag wire electrodes were introduced to measure the real-time electronic properties. The bending angle was controlled by adjusting the distance of the *z*-axis through the computer program.

Supporting Information

Supporting Information is available from the Wiley Online Library or from the author.

Acknowledgements

This work was supported by the Beijing Natural Science Foundation (Grant No. IS23040). The volunteers took part in the experiments involving wearables following informed consent.

Conflict of Interest

The authors declare no conflict of interest.

Author Contributions

D.W. and Z.L.W. proposed the idea and supervised the whole project. D.W., F.Y.Y., and P.G.P. designed the project and experiments. P.G.P. performed materials synthesis, ink development, and characterization experiments and analyzed the data. P.G.P. and F.Y.Y. fabricated the printed devices and performed the circuit design and measurements. All the authors discussed the results and commented on the manuscript. D.W. and P.G.P. wrote this paper.

Data Availability Statement

The data that support the findings of this study are available from the corresponding author upon reasonable request.

Keywords

disposable electronics, integratable, iontronics, osmotic energy, TENG

Received: July 22, 2023
Revised: August 15, 2023
Published online: September 24, 2023

[1] Y. Jeon, H.-R. Choi, J. H. Kwon, S. Choi, K. M. Nam, K.-C. Park, K. C. Choi, *Light. Sci. Appl.* **2019**, *8*, 114.
[2] X. Peng, K. Dong, C. Ye, Y. Jiang, S. Zhai, R. Cheng, D.i Liu, X. Gao, J. Wang, Z. L. Wang, *Sci. Adv.* **2020**, *6*, eaba9624.
[3] T. Someya, Z. Bao, G. G. Malliaras, *Nature* **2016**, *540*, 379.
[4] R. F. Service, *Science* **2003**, *301*, 909.
[5] Q. Yang, Z. Hu, M.-H. Seo, Y. Xu, Y. Yan, Y.-H. Hsu, J. Berkovich, K. Lee, T.-L. Liu, S. Mcdonald, H. Nie, H. Oh, M. Wu, J.-T. Kim, S. A. Miller, Y. Jia, S. Butun, W. Bai, H. Guo, J. Choi, A. Banks, W. Z. Ray, Y. Kozorovitskiy, M. L. Becker, M. A. Pet, M. R. Macewan, J.-K. Chang, H. Wang, Y. Huang, J. A. Rogers, *Nat. Commun.* **2022**, *13*, 6518.
[6] H. Lee, C. Song, Y. S. Hong, M. S. Kim, H. R. Cho, T. Kang, K. Shin, S. H. Choi, T. Hyeon, D.-H. Kim, *Sci. Adv.* **2017**, *3*, e1601314.
[7] Y. H. Jung, J.-Y. Yoo, A. Vázquez-Guardado, J.-H. Kim, J.-T. Kim, H. Luan, M. Park, J. Lim, H.-S. Shin, C.-J. Su, R. Schloen, J. Trueb, R. Avila, J.-K. Chang, D. S. Yang, Y. Park, H. Ryu, H.-J. Yoon, G. Lee, H. Jeong, J. U. Kim, A. Akhtar, J. Cornman, T.-I. Kim, Y. Huang, J. A. Rogers, *Nat. Electron.* **2022**, *5*, 374.
[8] D. Tobjörk, R. Österbacka, *Adv. Mater.* **2011**, *23*, 1935.
[9] X. Wang, X. Lu, B. Liu, D. Chen, Y. Tong, G. Shen, *Adv. Mater.* **2014**, *26*, 4763.
[10] L. Li, Z. Wu, S. Yuan, X.-B. Zhang, *Energy Environ. Sci.* **2014**, *7*, 2101.
[11] B. Yao, J. Zhang, T. Kou, Y. Song, T. Liu, Y. Li, *Adv. Sci.* **2017**, *4*, 1700107.
[12] A. C. Siegel, S. T. Phillips, M. D. Dickey, N. Lu, Z. Suo, G. M. Whitesides, *Adv. Funct. Mater.* **2010**, *20*, 28.
[13] S. Conti, L. Pimpolari, G. Calabrese, R. Worsley, S. Majee, D. K. Polyushkin, M. Paur, S. Pace, D. H. Keum, F. Fabbri, G. Iannaccone, M. Macucci, C. Coletti, T. Mueller, C. Casiraghi, G. Fiori, *Nat. Commun.* **2020**, *11*, 3566.
[14] Y. Shao, L. Wei, X. Wu, C. Jiang, Y. Yao, B.o Peng, H. Chen, J. Huangfu, Y. Ying, C. J. Zhang, J. Ping, *Nat. Commun.* **2022**, *13*, 3223.
[15] A. Asadpoordarvish, A. Sandström, C. Larsen, R. Bollström, M. Toivakka, R. Österbacka, L. Edman, *Adv. Funct. Mater.* **2015**, *25*, 3238.
[16] J.-H. Kim, S. Mun, H.-U. Ko, G.-Y. Yun, J. Kim, *Nanotechnology* **2014**, *25*, 092001.
[17] P.-K. Yang, Z.-H. Lin, K. C. Pradel, L. Lin, X. Li, X. Wen, J.-H. He, Z. L. Wang, *ACS Nano* **2015**, *9*, 901.
[18] T. C. Shyu, P. F. Damasceno, P. M. Dodd, A. Lamoureux, L. Xu, M. Shlian, M. Shtein, S. C. Glotzer, N. A. Kotov, *Nat. Mater.* **2015**, *14*, 785.

[19] C. Wu, X. Wang, L. Lin, H. Guo, Z. L. Wang, *ACS Nano* **2016**, *10*, 4652.
[20] Y. Liang, H. Dong, D. Aurbach, Y. Yao, *Nat. Energy* **2020**, *5*, 646.
[21] W. Shen, K. Li, Y. Lv, T. Xu, D. Wei, Z. Liu, *Adv. Energy Mater.* **2020**, *10*, 1904281.
[22] H. Li, C. Han, Y. Huang, Y. Huang, M. Zhu, Z. Pei, Q.i Xue, Z. Wang, Z. Liu, Z. Tang, Y. Wang, F. Kang, B. Li, C. Zhi, *Energy Environ. Sci.* **2018**, *11*, 941.
[23] X. Xiao, X. Xiao, Y. Zhou, X. Zhao, G. Chen, Z. Liu, Z. Wang, C. Lu, M. Hu, A. Nashalian, S. Shen, K. Xie, W. Yang, Y. Gong, W. Ding, P. Servati, C. Han, S. X. Dou, W. Li, J. Chen, *Sci.Adv* **2021**, *7*, eabl3742.
[24] X. Chu, G. Chen, X. Xiao, Z. Wang, T. Yang, Z. Xu, H. Huang, Y. Wang, C. Yan, N. Chen, H. Zhang, W. Yang, J. Chen, *Small* **2021**, *17*, e2100956.
[25] C. Wu, X. Lu, L. Peng, K. Xu, X. Peng, J. Huang, G. Yu, Y. Xie, *Nat. Commun.* **2013**, *4*, 2431.
[26] S. S. Afzal, W. Akbar, O. Rodriguez, M. Doumet, U. Ha, R. Ghaffarivardavagh, F. Adib, *Nat. Commun.* **2022**, *13*, 5546.
[27] J. Lv, L. Yin, X. Chen, I. Jeerapan, C. A. Silva, Y. Li, M. Le, Z. Lin, L. Wang, A. Trifonov, S. Xu, S. Cosnier, J. Wang, *Adv. Funct. Mater.* **2021**, *31*, 2102915.
[28] B. C. De, W. Zhang, C. Yang, A. Mándi, C. Huang, L. Zhang, W. Liu, M. W. Ruszczycky, Y. Zhu, M. Ma, G. Bashiri, T. Kurtán, H.-W. Liu, C. Zhang, *Nat. Commun.* **2022**, *13*, 7405.
[29] Y. Hui, Y. Yao, Q. Qian, J. Luo, H. Chen, Z. Qiao, Y. Yu, L. Tao, N. Zhou, *Nat. Electron.* **2022**, *5*, 893.
[30] S.-C. Yang, T.-Y. Lin, M. Ochoa, H. Lai, R. Kothandaraman, F. Fu, A. N. Tiwari, R. Carron, *Nat. Energy* **2023**, *8*, 40.
[31] X. Chen, D. Goodnight, Z. Gao, A. H. Cavusoglu, N. Sabharwal, M. Delay, A. Driks, O. Sahin, *Nat. Commun.* **2015**, *6*, 7346.
[32] J. Han, N. Xu, J. Yu, Y. Wang, Y. Xiong, Y. Wei, Z. L. Wang, Q. Sun, *Energy Environ. Sci.* **2022**, *15*, 5069.
[33] Q. Yang, T.-L. Liu, Y. Xue, H. Wang, Y. Xu, B. Emon, M. Wu, C. Rountree, T. Wei, I. Kandela, C. R. Haney, A. Brikha, I. Stepien, J. Hornick, R. A. Sponenburg, C. Cheng, L. Ladehoff, Y. Chen, Z. Hu, C. Wu, M. Han, J. M. Torkelson, Y. Kozorovitskiy, M. T. A. Saif, Y. Huang, J.-K. Chang, J. A. Rogers, *Nat. Electron.* **2022**, *5*, 526.
[34] K. Xiao, L. Jiang, M. Antonietti, *Joule* **2019**, *3*, 2364.
[35] Z. Zhang, L. Wen, L. Jiang, *Nat. Rev. Mater.* **2021**, *6*, 622.
[36] L. Yang, F. Yang, X. Liu, K. Li, Y. Zhou, Y. Wang, T. Yu, M. Zhong, X. Xu, L. Zhang, W. Shen, D. Wei, *Proc. Natl. Acad. Sci. U. S. A.* **2021**, *118*, e2023164118.
[37] D. Wei, F. Yang, Z. Jiang, Z. Wang, *Nat. Commun.* **2022**, *13*, 4965.
[38] K. Raidongia, J. Huang, *J. Am. Chem. Soc.* **2012**, *134*, 16528.
[39] J. Shen, Y. Cai, C. Zhang, W. Wei, C. Chen, L. Liu, K. Yang, Y. Ma, Y. Wang, C.-C. Tseng, J.-H. Fu, X. Dong, J. Li, X.-X. Zhang, L.-J. Li, J. Jiang, I. Pinnau, V. Tung, Y. Han, *Nat. Mater.* **2022**, *21*, 1183.
[40] G. Xue, Y. Xu, T. Ding, J. Li, J. Yin, W. Fei, Y. Cao, J. Yu, L. Yuan, L. Gong, J. Chen, S. Deng, J. Zhou, W. Guo, *Nat. Nanotechnol.* **2017**, *12*, 317.
[41] X. Tang, H. Zhou, Z. Cai, D. Cheng, P. He, P. Xie, D.i Zhang, T. Fan, *ACS Nano* **2018**, *12*, 3502.
[42] Y. Liu, B. Zhang, Q. Xu, Y. Hou, S. Seyedin, S. Qin, G. G. Wallace, S. Beirne, J. M. Razal, J. Chen, *Adv. Funct. Mater.* **2018**, *28*, 1706592.
[43] Y. Chao, Y. Ge, Z. Chen, X. Cui, C. Zhao, C. Wang, G. G. Wallace, *ACS Appl. Mater. Interfaces* **2021**, *13*, 7285.
[44] D. Akinwande, N. Petrone, J. Hone, *Nat. Commun.* **2014**, *5*, 5678.
[45] A. D. Franklin, *Science* **2015**, *349*, aab2750.
[46] R. J. Moon, A. Martini, J. Nairn, J. Simonsen, J. Youngblood, *Chem. Soc. Rev.* **2011**, *40*, 3941.
[47] A. Russo, B. Y. Ahn, J. J. Adams, E. B. Duoss, J. T. Bernhard, J. A. Lewis, *Adv. Mater.* **2011**, *23*, 3426.
[48] A. W. Martinez, S. T. Phillips, M. J. Butte, G. M. Whitesides, *Angew. Chem. Int. Ed. Engl.* **2007**, *46*, 1318.
[49] R. Derda, A. Laromaine, A. Mammoto, S. K. Y. Tang, T. Mammoto, D. E. Ingber, G. M. Whitesides, *Proc. Natl. Acad. Sci. U. S. A.* **2009**, *106*, 18457.